Measuring changes in inductance with microstrip resonators

R. M. Lewis, M. David Henry, Travis P. Young, M. P. Frank, M. A. Wolak, and Nancy Missert

Abstract— We measure the frequency dependence of a niobium microstrip resonator as a function of temperature from 1.4 to 8.4 K. In a two-micron wide half-wave resonator, we find the frequency of resonance changes by a factor of 7 over this temperature range. From the resonant frequencies, we extract inductance per unit length, characteristic impedance, and propagation velocity (group velocity). We discuss how these results relate to superconducting electronics. Over the 2 K to 6 K temperature range where SCE circuits operate, inductance shows a 19 % change and both impedance and propagation velocity show an 11 % change.

Index Terms—Superconducting materials, Kinetic inductance, Superconducting electronics, Nb, Superconducting resonators

I. INTRODUCTION

Superconducting electronics (SCE) is a blossoming field that aims to build logic circuits using Josephson junctions as the switching elements and superconducting wiring to create inductors and interconnects [1]. Because SCE circuits encode data using flux quanta, inductances are critical design parameters. However, many factors affect inductance including film composition, geometry, and temperature. Even with chips immersed in a helium bath, changes in elevation produce ~ 0.2 K variations in chip temperature. Cryocoolers can cool chips further down to ~ 2.7 K. Dense circuits may have hot spots. As SCE design methodologies advance and make use of modern electronic design aids [2] incorporating a detailed understanding of inductance into circuit design will result in more robust circuits with larger margins.

In this paper, we discuss measurements of inductance of sputtered niobium, Nb, films using a microstrip resonator. This method has been used in the past and is robust enough to be a basis for extracting London penetration depth, λ, measurements of superconducting films [3]. Superconducting circuits also use microstrip like structures for passive transmission line interconnects (PTLs) [4,5,6,7]. Our measurement shows that the inductance of our films is a strong function of temperature above ~ 6

K, but displays some temperature dependence even below 4 K. These inductance changes are understood as due to variations in λ with temperature, leading to a change in the kinetic inductance of the Nb film.

We also extract quality factors, Q, of the resonance. We find that the internal Q, $Q_{in} \approx 400$ at 4 K for our 3.5 GHz resonator and has a strong gradient with temperature. This indicates that in the push for energy efficient SCE circuits [8,9,10], losses in clock lines and PTLs, should not be neglected.

II. SAMPLE FABRICATION

An example of our half-wave microstrip resonator is shown in Fig. 1a, bonded to a test board. Samples were fabricated in Sandia's niobium (Nb) tantalum-nitride (Ta$_x$N) Josephson junction process although the microstrip does not contain any Josephson junctions. Further details on the Nb deposition [12] and the Ta$_x$N have been given elsewhere [13]. This is a two-layer process where the first metal deposition sputters a Nb/Ta$_x$N/Nb trilayer onto oxidized 150 mm silicon wafers at room temperature.
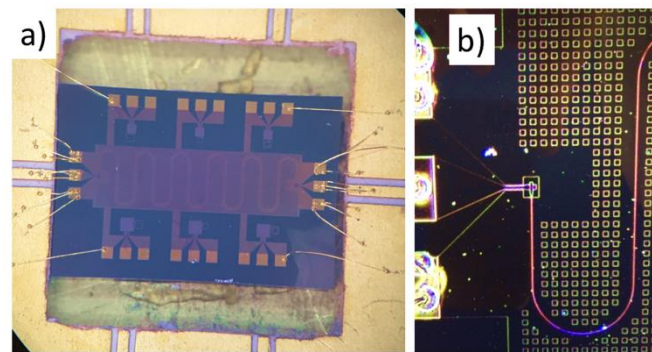

Fig.1. a) Microstrip resonator chip bonded into measurement board. The chip is approximately 6 mm long and 4 mm high. b) Coplanar microwave feed and parallel plate coupling capacitor. Square are flux trapping moats in ground plane.

R. M. Lewis is with the Quantum Phenomena group at Sandia National Laboratories, Albuquerque, NM 87123, USA, (e-mail: rmlewi@sandia.gov).

M. David Henry is with the MESA III-V Hetero-Integration facility at Sandia National Laboratories, Albuquerque, NM 87123, USA, (e-mail: mdhenry@sandia.gov).

M. P. Frank is with the Cognitive and Emerging Computing group at Sandia National Laboratories, Albuquerque, NM 87123 USA, (e-mail: mpfrank@sandia.gov).

M. A. Wolak is with the Nanoscale Sciences Department at Sandia National Laboratories, Albuquerque, NM 87123, USA, (e-mail: mwolak@sandia.gov).

Nancy Missert is with the Nanoscale Sciences Department Sandia National Laboratories, Albuquerque, NM 87123 USA, (e-mail: namisse@sandia.gov).

Color versions of one or more of the figures in this paper are available online at http://ieeexplore.ieee.org.

This layer includes a thin 5 nm aluminum (Al) etch stop layer embedded in the base electrode. The second metal deposition is a Nb wiring hook up layer. To fabricate the microstrip resonator, the trilayer stack is etched down to the Nb base electrode, stopping on the Al etch stop layer. This leaves approximately 200 nm of Nb with a thin 5 nm Al cap which forms the ground plane of the microstrip structure. An SiO_2 interlayer dielectric is then deposited at 250 °C and chemically-mechanically polished down to 200 nm, the level of the Nb counter-electrode in the trilayer structure. The top wiring layer is subsequently deposited and etched to yield a 2 μm wide, 200 nm thick line approximately 15.71 mm in length. The resonator is coupled to a coplanar waveguide feed line at each end through a parallel plate capacitor of approximately 45 fF. The coplanar microwave feed transitioning to a 20 μm by 12 μm parallel plate coupling capacitor is shown in Fig. 1b. Measurements of capacitance test structures fabricated nearby yield $C_0 = 0.188$ fF/μm^2 specific capacitance.

III. RESULTS

Fig. 2 shows broad-band microwave transmission (S_{21}) measurements from 1 GHz to 6 GHz of the micro-strip resonator at 4 K (blue), 6 K (red) and 7 K (yellow). The data were measured with a vector network analyzer in a probe equipped with a Lakeshore thermometer positioned close to the sample. Measurements used low microwave power to avoid heating the sample, allowing the temperature to be adjusted by lowering or raising the probe in the He vapor above the liquid. Three features are evident from these data. First, the frequency of resonance decreases as temperature increases. Second, transmission is lower on resonance for higher temperatures, indicating a change in impedance. Third, the width of the resonance measured 3 dB below peak transmission is narrowest at the lowest temperature indicating lower losses and higher Q.

Fig. 3 plots the resonant frequency, f_{pk}, versus temperature, T, between 1.4 K and 8.35 K. This plot combines data measured in a 1 K pot cryostat and in the 4 K dip probe. In both cases, the sample was mounted in vapor and is in good thermal equilibrium with the thermometer. Errors in temperature are smaller than the symbol size. Measurements were performed in a 500 MHz band around resonance with $P_{inc} \approx -40$ dBm incident on the sample, sufficiently low that reducing power further didn't narrow the resonance. Resonant frequencies are determined to better than 1 MHz.

The f_{pk} versus T data track the development of the superconducting state closely as the sample is cooled. f_{pk} saturates at low temperature, $T = 1.41$ K, at about 3.502 GHz. At $T = 8.35$ K, f_{pk} = 591 MHz—nearly 7 times lower than at 1.4 K. Our Nb films consistently show T_c of 8.4 K. No data was recorded above T_c, as transmission is weak owing to the high surface resistance of Nb in the normal state.

A subset of these data were fit to determine the internal and loaded quality factors of the resonator, Q_{in} and Q_L respectively. Here Q_L is the loading on the resonator due to the 50 Ohm environment of the measurement leads, while Q_{in} is due to losses

in the resonator, such as finite temperature losses in the superconducting Nb film. The fitting function is [13];

$$S_{21} = \frac{-Q_T}{2Q_L} - \frac{Q_T}{2Q_L} \frac{\left(\left(\frac{1}{Q_T}\right)^2 - \left(\frac{\omega}{\omega_0} - \frac{\omega_0}{\omega}\right)^2 - 2i\left(\frac{\omega}{\omega_0} - \frac{\omega_0}{\omega}\right)\frac{1}{Q_T}\right)}{\left(\frac{1}{Q_T}\right)^2 + \left(\frac{\omega}{\omega_0} - \frac{\omega_0}{\omega}\right)^2}$$
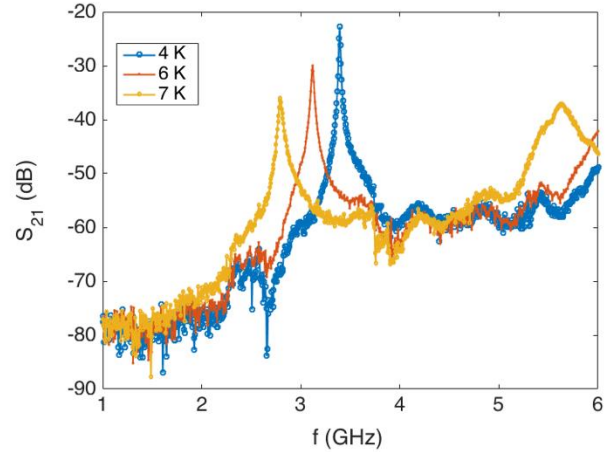

Fig. 2. Microwave transmission measurements of the Nb microstrip resonator at 4 K, 6 K, and 7 K.

where $\omega = 2\pi f$, is the angular frequency, $\omega_0 = 2\pi f_{pk}$, and $Q_T^{-1} = Q_L^{-1} + Q_{in}^{-1}$. These data show Q_{in} increasing steadily from ~20 at 8 K, the highest T dataset that was fit-able, to 1210 ± 50 at 1.4 K although Q_{in} has still not completely saturated. Notably, $Q_{in} \approx 400$ at 4 K and shows a strong temperature dependence. Extrapolating to frequencies ~100 GHz, where the wavelength is ~ 1 mm, requires taking the frequency dependence of the attenuation into account. Solutions for scaling attenuation are available from the two-fluid model and the Mattis-Bardeen model
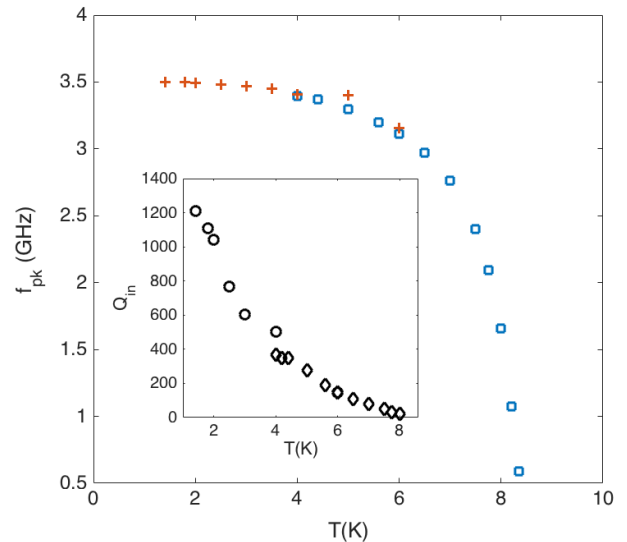

Figure 3. Resonant frequency f_{pk} versus temperature T. Blue squares show data obtained in the dipping probe, red + show data obtained in the 1 K pot cryostat. Inset: Internal quality factor Q_{in} versus T.

[5]. The two-fluid model predicts attenuation scales $\sim \omega^2$ for all ω. The more realistic Mattis-Bardeen model [5] predicts attenuation $\sim \omega^2$ for $\omega << \Delta$ but for frequencies nearer the gap attenuation scales more like $\sim \omega$. This suggests the Q_{in} will drop proportionate $\sim \omega^{-1}$ or by approximately 30 to 100 for f $\sim$ 100 GHz. Since Q represents the fractional attenuation of the signal per wavelength of propagation, we expect SFQ signals will propagate $\sim Q$ wavelengths. Since $Q_{in = 400}$, even scaling attenuation up by 100x would allow $\sim$ 4 mm of signal propagation. This level of loss would not degrade cross chip signal transmissions using PTLs. For clock frequencies closer to 10 GHz, losses in this Nb at $\sim$ 4 K due to residual surface resistance are low, but not negligible. However, since clock lines can carry significant power, fractions of a dB should be accounted for. Finally, the strong gradient of Q_{in} with T means local warming will exacerbate losses.

IV. DISCUSSION

The strong dependence of f_{pk} on T is tied to the large kinetic inductance of the microstrip line. Geometry and the resonator length suggest resonance would occur at $f_g \approx 5.4$ GHz if the Nb film were a lossless metal that *did not* exhibit kinetic inductance, L_k. The kinetic inductance fraction [14] of the Nb line, $\alpha = 1 - (f_{pk}/f_g)^2 \approx 0.58$ at 1.4 K, is much higher than expected for Nb. Correspondingly, the characteristic impedance of the line is higher, $Z = 24$ Ohms, and the propagation velocity of light is lower, $v_p = 0.36 c$ than would be the case in the absence of L_k, where c is the speed of light in vacuum.
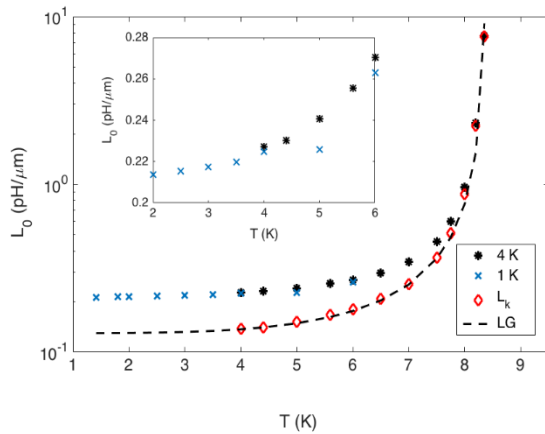

Fig. 4. Inductance per unit length, L_0, extracted from f_{pk} measurements. The asterisks (*) were measured in a 4 K dip probe. The X (X) are data measured in a 1 K pot cryostat. Diamonds are L_0 data minus the geometric inductance determined at 1.4 K. The dashed line is calculated using Landau-Ginzburg theory. **Inset:** Linear scale plot of L_0 between 2 K and 6 K.

The inductance per unit length, L_0 in pH/µm, is plotted against T in Fig. 4. The values of L_0 were calculated from the f_{pk} vs. T data in Fig. 3 as follows; the signal propagation velocity, $v_p = 2 l f_{pk}$, where, on resonance, the wavelength equals twice the length of the resonator, l. Then, $L_0 = C_0^{-1} v_p^{-2}$, and $C_0 = 0.188$ fF/µm^2 is measured from capacitance test structures on the same wafer at room temperature and is assumed

temperature independent. The coupling capacitances change the effective length of the resonator slightly and have been accounted for. At the lowest temperature of 1.4 K, $L_0 = 0.215$ pH/µm but rises rapidly with T to 7.68 pH/µm at 8.35 K.

Fig. 4 also shows the calculated kinetic inductance per unit length (dashed line) using the Landau-Ginzburg (LG) derived equation, $L_k = \mu_0 \lambda^2/A$ where A is the cross sectional area of the micro-strip transmission line and μ_0 is the permeability of free space. The standard LG form [15] for the temperature dependence of the London penetration depth, $\lambda(T) = \lambda_0/\sqrt{1 - (T/T_C)^4}$ is used where $T_c = 8.38$ K is used and $\lambda_0 = 180$ nm provides a good match to our Nb. The somewhat large λ_0 is supported by examining in plane magnetic field dependence of Josephson junctions made in this process. $\lambda_{0*} = 90$ nm is a typical number reported for Nb thin films [16], indicating that our Nb is somewhat atypical. Note that the L_k curve is not a rigorous fit to our data, but matches the extracted L_k well. L_k is determined by subtracting the geometric inductance, $L_g = (1-\alpha) L_0$ at 1.4 K, from the raw L_0 and is shown by diamond symbols on Fig.4. Also, changing λ_0 moves the calculated LG curve shown in Fig. 4 up or down but doesn't change its shape. Lower values of λ_0 would thus give lower α and are less sensitive to temperature.

A possible factor in the large observed α could be the Al etch stop layer used in our fabrication process. The Al etch stop layer allows reliable etching of Josephson junctions from the Nb\Ta$_x$N\Nb trilayer deposition. In this micro-strip resonator, Al forms the surface of the ground plan and so any unoxidized Al will be only a proximity superconductor at 4 K, and thus contribute to a large L_k and lower Q_{in}.
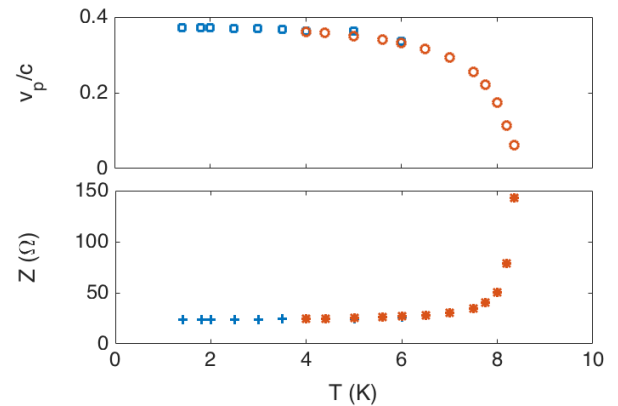

Fig. 5. **Upper panel:** Signal propagation velocity, v_p/c versus T. Lower panel: impedance, Z versus T. Both data sets are calculated from f_{pk} data in Fig.3.

Inductance is a key design parameter in SFQ circuits. Inductance fluctuations can change the way a circuit works and should be taken into account in design. The inset of Fig. 4 plots the data in the range from 2 to 6 K around a probable 4 K working point. We see a change in L_0 from 0.21 pH/µm at 1.4 K to 0.27 pH/µm at 6 K, a change of 19 %. Considering that SCE could run on a cryocooled system at $\sim$ 3 K or in helium at $\sim$ 4.2 K, such variations should be allowed for in the design process, although the range between 3 and 5 K shows a smaller 9 %

This article has been accepted for publication in a future issue of this journal, but has not been fully edited. Content may change prior to final publication. Citation information: DOI 10.1109/TASC.2019.2899867, IEEE Transactions on Applied Superconductivity

4

variation. Finally, it is worth noting that the value of L_0 found here at 1.4 K is close to that calculated by Chang [17].

The large change in the inductance of the Nb microstrip line is also reflected in other important electronic parameters. Fig. 5, shows the characteristic impedance of the line, Z, in the lower panel. $Z = (L_0/C_0)^{1/2} = (1/C_0^2 v_p^2)^{1/2}$ is calculated from the data in Fig. 3 where $C_0 = 0.188$ fF/μm^2. A slower variation of Z from 23.8 Ohms to 26.8 Ohms occurs across the 2 K to 6 K application range. The propagation velocity as a fraction of the speed of light, v_p/c, is plotted in the upper panel of Fig. 5. v_p drops from 0.37 c to 0.33 c between 2 K and 6 K. Assuming v_p at 3.5 GHz can be extrapolated to SFQ pulses at ~ 100 GHz, such variations should be noted because of the impact on signal timing when long transmission lines are used.

V. CONCLUSION

We have discussed measurements of Nb superconducting resonators as a function of temperature. We find that our Nb microstrip resonators shows dramatic reduction in resonant frequency as T increases towards T_c. This structure was used to extract inductance per unit length. We point out that the inductance shows a 9 % increase between 3 and 5 K and a significant (~19%) increase between 2 K and 6 K and that as inductance is a critical circuit parameter in SCE, such variations with temperature should be taken into account in cell libraries. Over the 2 to 6 K T range, both Z and v_p vary by 11 %. Nb films with shorter London penetration length, λ_0, higher T_c, or other superconducting films with higher T_c e.g., NbN or NbTiN would alleviate this problem and show less temperature sensitivity operating near 4 K. Finally, the losses in our Nb at 4 K at 3.5 GHz indicate signals propagate ~ 400 wavelengths during $1/e$ attenuation, much further than typical chip sizes. This number suggests that clock lines and ac bias lines, which carry significant power can deposit non-negligible heat into SCE chips. Low power SCE technologies and reversible computing technologies should account for this in their power budgets.

REFERENCES

[1] K. K. Likharev and V. K. Semenov, "RSFQ Logic/Memory Family: A New Josephson-Junction Technology for Sub-Terahertz-Clock-Frequency Digital Systems", IEEE Trans. Appl. Supercond. Vol. 1, No. **1**, 3 (1991).

[2] See IARPA's SuperTools program: https://www.iarpa.gov/index.php/newsroom/iarpa-in-the-news/2018/1085-iarpa-launches-supertools-program-to-develop-superconducting-circuit-design-tools

[3] B. W. Langley, S. M. Anlage, R. F. W. Pease, and M. R. Beasley, 'Magnetic penetration depth measurements of superconducting thin films by a microstrip resonator technique', Rev. Sci. Instrum. **62**, 1801 (1991).

[4] R. L. Kautz, 'Miniaturization of Normal-State and Superconducting Striplines', Journal of Research of the National Bureau of Standards, Vol. **84**, No. 3, 247 (1979).

[5] R. L. Kautz, 'Picosecond pulses on superconducting striplines', Journal of Applied Physics **49**, 308 (1978); doi: 10.1063/1.324387

[6] S. V. Polonsky, V. K. Semenov, and D. F. Schneider, 'Transmission of Single-Flux-Quantum Pulses Along Superconducting Microstrip Lines', IEEE Trans. Appl. Supercond. Vol. **3**, No. 1, 2598 (1993).

[7] Kasumi Takagi, Masamisu Tanaka, Shingo Iwasaki, Ryo Kasagi, Irina Kataeva, Shuichi Nagasawa, Tesuro Satoh, Hiroyuki Akaike, and Akira Fujimaki, 'SFQ Propagation Properties in Passive Transmission Lines Based on a 10-Nb-Layer Structure', IEEE Trans. Appl. Supercond. Vol. **19**, No. 3, 617 (2009).

[8] D. E. Kirichenko, S. Sarwana, and A. F. Kirichenko, 'Zero Static Power Dissipation Biasing of RSFQ Circuits', IEEE Trans. Appl. Supercond. IEEE Trans. Appl. Supercond., vol. **21**, no. 3, pp. 776-779, (2011).

[9] Quentin P. Herr, Anna Y. Herr, Oliver T. Olberg, and Alexander G. Ioannidis, "Ultra-low-power Superconductor Logic", J. Appl. Phys. **109**, 103903 (2011); doi: 10.1063/1.3585849

[10] Naoki Takeuchi, Dan Ozawa, Yuki Yamanashi and Nobuyuki Yoshikawa, 'An adiabatic quantum flux parametron as an ultra-low-power logic device', Supercond. Sci. Technol. **26**, 035010 (2013); doi:10.1088/0953-2048/26/3/035010

[11] M. D. Henry, S. Wolfley, T. Monson, B. G. Clark, E. Shaner, and R. Jarecki, "Stress dependent oxidation of sputtered niobium and effects on superconductivity," *Journal of Applied Physics,* Vol. **115**, no. 8, pp. 083903, (2014).

[12] N. Missert, L. Brunke, M. D. Henry, S. Wolfley, S. Howell, J. Mudrick, and R. M. Lewis, 'Materials Study of NbN and TaxN Thin Films for SNS Josephson Junctions', IEEE Trans. Appl. Supercond. Vol. **27** , No. 4, 1100904 (2017); DOI: 10.1109/TASC.2017.2669582

[13] B. A. Mazin, Ph.D. dissertation, California Institute of Technology, 2004.

[14] J. Gao, J. Zmuidzinas, B. A. Mazin, P. K. Day, and H. G. Leduc, "Experimental study of the kinetic inductance fraction of superconducting coplanar waveguide", Physics Research A **559**, 585-587 (2006).

[15] Michael Tinkham, 'Introduction to Superconductivity, 2nd Ed.', Dover Publications, Inc., Mineola, NY, (1996).

[16] Sergey K. Tolpygo, Vladimir Bolkhovsky, T. J. Weir, C. J. Galbraith, Leonard M. Johnson, Mark A. Gouker, and Vasili K. Semenov, 'Inductance of Circuit Structures for MIT LL Superconductor Electronics Fabrication Process With 8 Niobium Layers', IEEE Trans. Appli. Supercond. Vol. **25**, No. 3, 1100905 (2015); DOI: 10.1109/TASC.2014.2369213

[17] W. H. Chang, 'The inductance of a superconducting strip transmission line', Journal of Applied Physics **50**, 8129 (1979); doi: 10.1063/1.325953